



Chladni Figures: A Mathematical Exploration of Visual Music

Evan Quistad

Realgymnasium Rämibühl

Advisor: Yee Ling Willems-Ong

January 1, 2022

Abstract

Inspired by the formation and applications of Chladni figures on violin plates, this paper aims to further my understanding of how Chladni figures form by constructing a mathematical and physical model myself. Armed only with the book “Elementary Differential Equations and Boundary Value Problems (W. Boyce and R. DiPrima, 1986)”, from which the vast majority of my knowledge on this subject stems, my father’s workshop as well as the school’s science lab, I set out on the mission to explore and solve the two dimensional partial differential wave equation on my own. The methods in this paper are not necessarily conventional, since they were largely obtained through hours of trial and error.

As I have always been fascinated by how mathematics is used to describe physical and natural phenomena, one main goal for this paper is to document my personal mathematical journey. I have therefore presented a large portion of the mathematics in the main body of the paper.

Contents

1	A Brief Explanation of Chladni Figures	3
2	Derivation of the Two Dimensional Wave Equation	6
3	Chladni Figures on a Rectangular Plate	9
3.1	Boundary Conditions for a Rectangular Plate	9
3.2	Solving the Wave Equation for a Rectangular Plate	10
4	Nodes on a Rectangular Plate	16
4.1	Nodes in the x Direction	16
4.2	Nodes in the y Direction	17
4.3	Nodes in the t Direction	17
5	Chladni Figures on a Circular Plate	19
5.1	Boundary Conditions for a Circular Plate	19
5.2	Solving the Wave Equation for a Circular Plate	21
5.3	Nodes on a Circular Plate	23
5.4	t - Nodes on a Circular Plate	24
6	Polar Form of the Two Dimensional Wave Equation	29
7	Application of the Polar Wave Equation on a Circular Plate	33
8	Lessons from the Mathematics	37
9	Experimental Results	39
9.1	Results from the Circular Membrane	41
9.2	Results from the Rectangular Membrane	43
10	Chladni Figures in Lutherie	44
11	Conclusion and Improvements	46
12	Personal Reflection	47

1 A Brief Explanation of Chladni Figures

When listening to a string instrument, the wave like nature of sound comes naturally. The notion of a vibrating string is one which we are accustomed to and therefore find inherently logical. However, when confronted with vibrations in higher dimensions, it is easy to become confused by the intricacy of the oscillations. Luckily, we can come up with a simple but effective method to help us understand the vibration of two dimensional surfaces, such as the back plate of a violin.

Chladni figures are a way to visualize the nodes of standing waves on a plate or membrane. They were first observed by Galileo in 1638 and later more rigorously explored by the 19th century German physicist and musician Ernst Chladni. By spreading a fine grain such as sand or salt on a brass plate and stroking the plate with a cello or bass bow, Chladni was able to show how the grain agglomerated in certain patterns known as modes. This happens because when a plate resonates, just like a string, there are certain points where the plate does not vibrate (node).

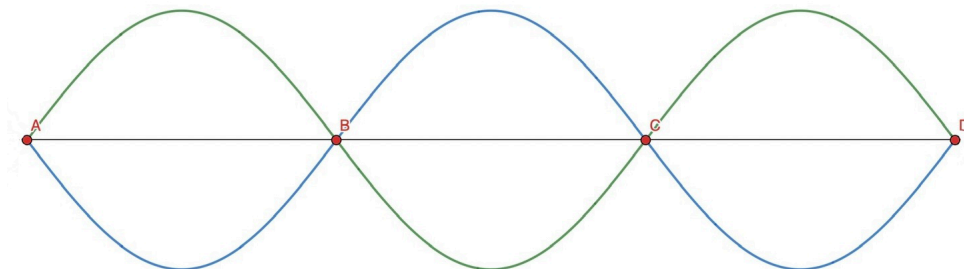


Figure 1: Vibration and nodes of a string

In the illustration above, the nodes are the points A, B, C and D. Extending this to a two dimensional, the fine grain would be pushed away from the high/low points (antinodes) and would build up at the nodes. When plates resonate, it is possible to create intricate patterns by using the method of Ernst Chladni.

Despite being able to visualize the patterns on a two dimensional plate, the necessary mathematics to describe and predict the modes was not available at the time. Having witnessed the production of these figures, Napoleon Bonaparte himself offered a prize for the best mathematical explanation of this phenomenon. After a first wave of unsuccessful attempts, the correct approach was finally discovered by the French mathematician and physicist Sophie Germain in 1816.

Apart from being a mathematical sensation, Germain also represents a benchmark for the involvement of women in the academic world.

Nowadays Chladni figures have a wide array of applications, most notably in the building of string instruments and quantum mechanics. As a violinist, I first heard of Chladni figures in the context of lutherie. When playing an instrument such as a violin, the front and back plates vibrate. Reminiscent of Chladni's original technique, a bow is used to set the plates in motion. This time however, the bow contacts the strings which are attached to the plate. The vibrations are carried through the bridge to the soundpost, which then in turn causes point driven excitations in the plates.

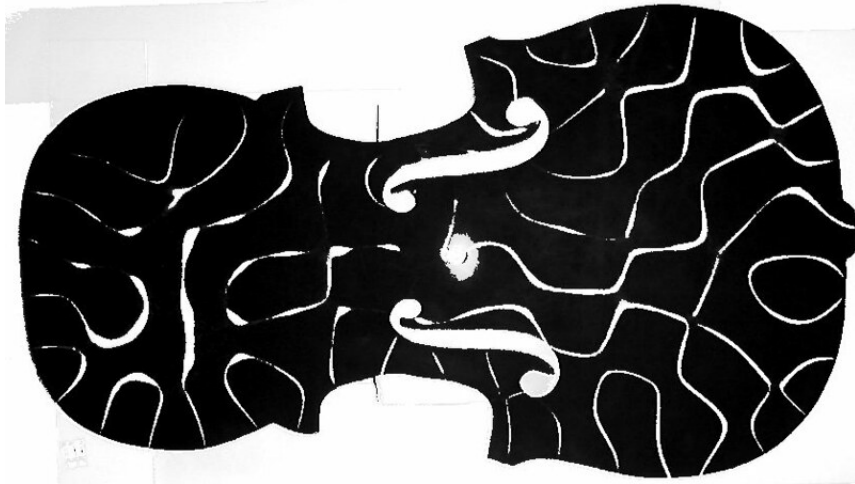


Figure 2: Chladni figures on a violin plate [3]

Similar to Chladni's experiments, the resonance of the plates form nodal patterns. However, since a violin is a closed body and one is not likely to spread a fine grain over it, the Chladni figures which a violin plate creates while being played are rarely noticed or recognized as a significant sign of a violin's acoustic quality. While there do not seem to be particular Chladni figures which are a sign for a good or bad violin, the Chladni figures a violin produces can tell a luthier some important information about the back plate of his instrument, as shall be discussed later in this paper.

To further understand how these figures form, it is of great utility to devise a mathematical model describing the phenomenon. For this paper we will use the two dimensional partial differential wave equation to predict the formation of Chladni figures. Since the violin's bottom plate is connected to the top plate along the edges by so called "ribs", for our model, we will assume that the edges of the membrane are fixed. This implies, that the amplitude of the vibration is equal to zero at all times along the borders.

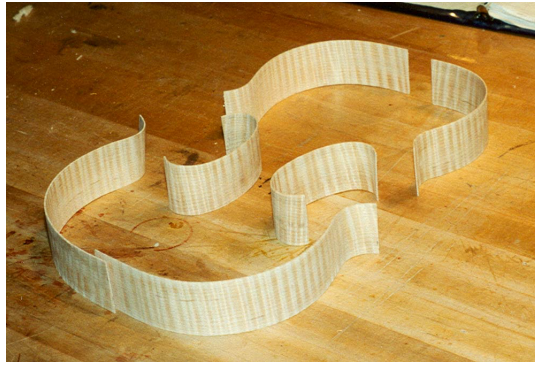


Figure 3: Violin ribs [4]

As I have discovered throughout the writing of this paper, the shape of the plate directly affects the shape of the Chladni figures. Unfortunately the shape of a violin's back plate is quite intricate. Additionally the plates are not two dimensional, since they are curved outward. These two very significant complications with the added fact that wood has a grain (and is therefore not isotropic) make obtaining a formula which consistently predicts the patterns virtually impossible. Only numerical solutions are plausible in this situation. However, since we are interested in analytical solutions in this paper, we must make appropriate simplifications to our physical system, the most important one being the shape of the plate. We will explore the figures on a circular and rectangular membrane with fixed borders, the other simplifications and assumptions will be explained in the following section.

2 Derivation of the Two Dimensional Wave Equation

We begin by looking at a small portion of a vibrating membrane. It is assumed that the membrane has no thickness, is fully elastic and is isotropic. We obtain the following system:

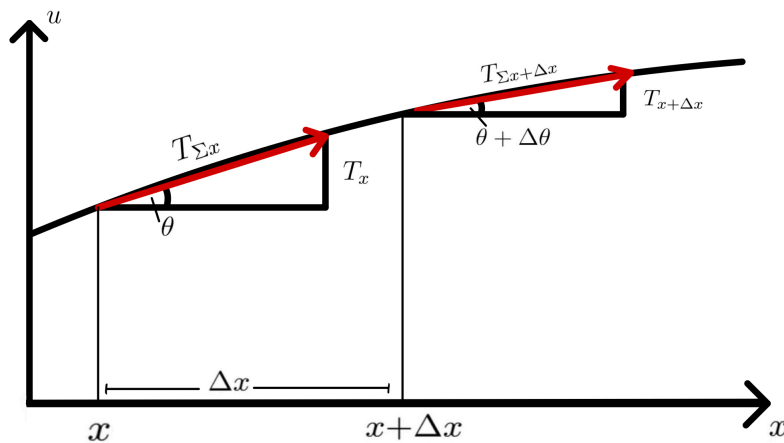


Figure 4: x-axis of our system

In the figure above, T is the tension force acting upon the membrane and the subscripts indicate in which direction the tension force is acting. Since for the y -axis, the sketch is exactly the same, only the x -axis of the system is shown in figure 4 for visualization purposes. Using the rules of trigonometry, it follows that

$$T_x = \sin(\theta) \cdot T_{\Sigma x} \quad (1)$$

and

$$T_y = \sin(\theta) \cdot T_{\Sigma y}. \quad (2)$$

Similarly we can also say that

$$T_{x+\Delta x} = \sin(\theta + \Delta\theta) \cdot T_{\Sigma x+\Delta x} \quad (3)$$

and

$$T_{y+\Delta y} = \sin(\theta + \Delta\theta) \cdot T_{\Sigma y+\Delta y}. \quad (4)$$

Since there is no horizontal acceleration in this system, we can now focus on the vertical acceleration of the membrane. The resulting tension force

acting upon the section Δx and Δy respectively is equal do the difference in the tension forces on each end. Hence

$$T_{x,res} = T_{x+\Delta x} - T_x \quad (5)$$

and

$$T_{y,res} = T_{y+\Delta y} - T_y. \quad (6)$$

According to Newtons second law of motion, $F = ma$, the sum of all forces is equal to mass times acceleration. We find that

$$T_{x,res} + T_{y,res} = T_{x+\Delta x} - T_x + T_{y+\Delta y} - T_y = ma. \quad (7)$$

Since mass is equal to linear density (ρ) times length (Δx) and acceleration is equal to the second derivative of position (u) with respect to time, we can rewrite equation (7) as

$$T_{x+\Delta x} - T_x + T_{y+\Delta y} - T_y = \rho \cdot \Delta x \cdot \frac{\partial^2 u}{\partial t^2}. \quad (8)$$

Inserting from equations (1) through (4) yields

$$\sin(\theta+\Delta\theta) \cdot T_{\Sigma x+\Delta x} - \sin(\theta) \cdot T_{\Sigma x} + \sin(\theta+\Delta\theta) \cdot T_{\Sigma y+\Delta y} - \sin(\theta) \cdot T_{\Sigma y} = \rho \cdot \Delta x \cdot \frac{\partial^2 u}{\partial t^2}. \quad (9)$$

By dividing by Δx on both sides, we obtain

$$\frac{\sin(\theta + \Delta\theta) \cdot T_{\Sigma x+\Delta x} - \sin(\theta) \cdot T_{\Sigma x} + \sin(\theta + \Delta\theta) \cdot T_{\Sigma y+\Delta y} - \sin(\theta) \cdot T_{\Sigma y}}{\Delta x} = \rho \cdot \frac{\partial^2 u}{\partial t^2}. \quad (10)$$

Since $\Delta x \approx \Delta y$ when the difference is small, equation (10) takes the form

$$\frac{\sin(\theta + \Delta\theta) \cdot T_{\Sigma x+\Delta x} - \sin(\theta) \cdot T_{\Sigma x}}{\Delta x} + \frac{\sin(\theta + \Delta\theta) \cdot T_{\Sigma y+\Delta y} - \sin(\theta) \cdot T_{\Sigma y}}{\Delta y} = \rho \cdot \frac{\partial^2 u}{\partial t^2}. \quad (11)$$

Because the derivative of a function is defined as $\lim_{\Delta x \rightarrow 0} \frac{f(x+\Delta x) - f(x)}{\Delta x}$, taking the limit as $\Delta x \rightarrow 0$ and $\Delta y \rightarrow 0$ gives us

$$T_x \cdot \frac{\partial(\sin \theta)}{\partial x} + T_y \cdot \frac{\partial(\sin \theta)}{\partial y} = \rho \cdot \frac{\partial^2 u}{\partial t^2}. \quad (12)$$

We can also approximate $\sin(\theta) \approx \tan \theta \approx \frac{du}{dx} \approx \frac{du}{dy}$, where u is the displacement of the membrane at that point, for small angles θ . We can therefore write

$$T_x \cdot \frac{\partial^2 u}{\partial x^2} + T_y \cdot \frac{\partial^2 u}{\partial y^2} = \rho \cdot \frac{\partial^2 u}{\partial t^2}. \quad (13)$$

Also, $T_x \approx T_y$ for small angles θ . Equation (13) takes the form

$$T \cdot \left(\frac{\partial^2 u}{\partial x^2} + \frac{\partial^2 u}{\partial y^2} \right) = \rho \cdot \frac{\partial^2 u}{\partial t^2}. \quad (14)$$

Dividing by ρ and letting $\frac{T}{\rho} = \alpha^2$ to facilitate future calculations, we finally obtain the two dimensional wave equation

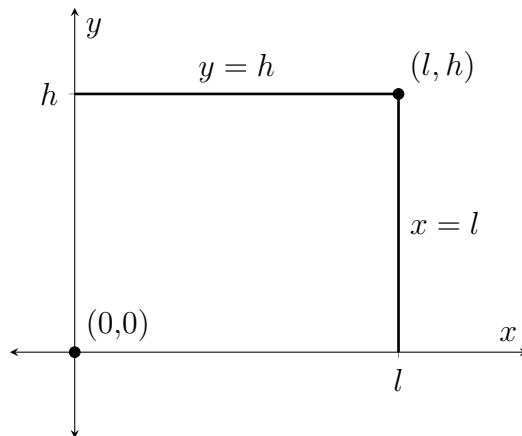
$$\frac{\partial^2 u}{\partial t^2} = \alpha^2 \left(\frac{\partial^2 u}{\partial x^2} + \frac{\partial^2 u}{\partial y^2} \right), \quad (15)$$

Where α^2 is equal to tension force over linear material density. Incidentally, α is also equal to the propagation speed of the wave in the material in m/s.

3 Chladni Figures on a Rectangular Plate

3.1 Boundary Conditions for a Rectangular Plate

We now wish to solve the wave equation for a rectangular plate with fixed ends.



We label the height of the plate in the y direction as h , and the length of the plate in x direction as l .

Since we know that the plate is fixed along its borders, we can set up the following boundary conditions:

$$u(0, y, t) = 0, \quad (16)$$

$$u(l, y, t) = 0, \quad (17)$$

$$u(x, 0, t) = 0, \quad (18)$$

$$u(x, h, t) = 0. \quad (19)$$

We also set the initial displacement to be 0 for all x and y at $t = 0$ and as such, get the last boundary condition

$$u(x, y, 0) = 0. \quad (20)$$

3.2 Solving the Wave Equation for a Rectangular Plate

We first begin with the wave equation derived in section 2:

$$\frac{\partial^2 u}{\partial t^2} = \alpha^2 \left(\frac{\partial^2 u}{\partial x^2} + \frac{\partial^2 u}{\partial y^2} \right). \quad (21)$$

We will first assume that $u(x, y, t)$ can be written as $X(x)Y(y)T(t)$. This method is named separation of variables, since we separate $u(x, y, t)$, which is a function of x , y and t , into three different functions X , Y and T , where each is dependent on one unique variable. Therefore, the two dimensional wave equation becomes

$$X(x)Y(y)T''(t) = \alpha^2 \left(X''(x)Y(y)T(t) + X(x)Y''(y)T(t) \right). \quad (22)$$

We can now factor out $T(t)$ to obtain

$$X(x)Y(y)T''(t) = \alpha^2 T(t) \left(X''(x)Y(y) + X(x)Y''(y) \right). \quad (23)$$

For simplicity, we will from now on use X , Y and T for $X(x)$, $Y(y)$ and $T(t)$ respectively. Furthermore, we can now divide the expression by XYT . Thus we write

$$\frac{T''}{T} = \alpha^2 \frac{X''}{X} + \alpha^2 \frac{Y''}{Y}. \quad (24)$$

We can rearrange this term to the form

$$\frac{T''}{T} - \alpha^2 \frac{Y''}{Y} = \alpha^2 \frac{X''}{X}. \quad (25)$$

Since both sides are equal, and not functions of the same variable, we can say that both sides must be equal to the same constant, which we will name σ . We have

$$\frac{T''}{T} - \alpha^2 \frac{Y''}{Y} = \sigma \quad (26)$$

and

$$\alpha^2 \frac{X''}{X} = \sigma. \quad (27)$$

We can rearrange equation (26) to obtain

$$\alpha^2 \frac{Y''}{Y} = \frac{T''}{T} - \sigma. \quad (28)$$

Since both sides are equal, these again must both be equal to the same constant, which we will name γ . Then

$$\frac{T''}{T} - \sigma = \gamma \quad (29)$$

and

$$\alpha^2 \frac{Y''}{Y} = \gamma. \quad (30)$$

Hence we can say

$$\frac{T''}{T} = \gamma + \sigma. \quad (31)$$

We now have three second order homogenous ordinary differential equations: (27), (30) and (31). We can now solve each one of these equations separately. Let us begin with equation (27). We can rearrange this ordinary differential equation to the form

$$\alpha^2 X'' - \sigma X = 0. \quad (32)$$

To avoid future complications, we will let $\sigma = -\lambda^2$. Equation (32) becomes

$$\alpha^2 X'' + \lambda^2 X = 0. \quad (33)$$

Now we assume that e^{rx} , where r is a constant, is a valid solution to equation (33). We can write

$$\alpha^2 r^2 e^{rx} + \lambda^2 e^{rx} = 0. \quad (34)$$

Dividing by e^{rx} on both sides yields

$$\alpha^2 r^2 + \lambda^2 = 0. \quad (35)$$

We can now easily solve equation (35) in respect to r using the quadratic formula $r = \frac{-b \pm \sqrt{b^2 - 4ac}}{2a}$, where $a = \alpha^2$, $b = 0$ and $c = \lambda^2$. Thus we find the following values for r :

$$r_1 = \frac{i\lambda}{\alpha}, \quad (36)$$

$$r_2 = -\frac{i\lambda}{\alpha}, \quad (37)$$

where i is the imaginary unit, such that $i^2 = -1$. We now know that both $e^{\frac{i\lambda}{\alpha}x}$ and $e^{-\frac{i\lambda}{\alpha}x}$ are solutions to equation (33). According to the superposition principle [1] we can say that any linear combination of these two linearly independent solutions will also be a solution of the equation. Thus, the general solution (ϕ) of $X(x)$ is

$$\phi(x) = c_1 e^{\frac{i\lambda}{\alpha}x} + c_2 e^{-\frac{i\lambda}{\alpha}x}. \quad (38)$$

Using the boundary condition (16), we can obtain the following equation from equation (38):

$$\phi(0) = c_1 e^0 + c_2 e^0 = 0. \quad (39)$$

Since $e^0 = 1$, we can say that

$$c_1 + c_2 = 0 \quad (40)$$

and thus

$$c_1 = -c_2. \quad (41)$$

Similarly, by using the boundary condition (17) on equation (38), we find that

$$\phi(l) = c_1 e^{\frac{i\lambda}{\alpha}l} + c_2 e^{-\frac{i\lambda}{\alpha}l} = 0. \quad (42)$$

This equation is valid for $c_1 = c_2 = 0$. However, using these constants would result in $u(x, y, t) = 0$ at all times for any x and y . This is clearly not an accurate description of the physical system, since Chladni figures would not form under these conditions. Therefore, since $c_1 = -c_2$, neither c_1 nor c_2 are allowed to be 0. This is only the case if

$$e^{\frac{i\lambda}{\alpha}l} - e^{-\frac{i\lambda}{\alpha}l} = 0. \quad (43)$$

We must now solve equation (43) with respect to λ . This can be done by first splitting λ into its real and imaginary parts. To do this, we let $\lambda = \mu + i\nu$. Equation (43) takes the form

$$e^{\frac{i\mu}{\alpha}l} e^{\frac{\nu}{\alpha}l} - e^{-\frac{i\mu}{\alpha}l} e^{-\frac{\nu}{\alpha}l} = 0. \quad (44)$$

Now, by using Euler's relation $e^{ikx} = \cos(kx) + i \sin(kx)$, where k is a real valued constant, as well as the fact that $\cos(-x) = \cos(x)$ and $\sin(-x) = -\sin(x)$, we find that equation (44) becomes

$$\left(\cos\left(\frac{\mu l}{\alpha}\right) + i \sin\left(\frac{\mu l}{\alpha}\right) \right) e^{\frac{\nu}{\alpha} l} - \left(\cos\left(\frac{\mu l}{\alpha}\right) + i \sin\left(\frac{\mu l}{\alpha}\right) \right) e^{-\frac{\nu}{\alpha} l} = 0. \quad (45)$$

This term can be rearranged to the form

$$\cos\left(\frac{\mu l}{\alpha}\right) \left(e^{\frac{\nu}{\alpha} l} - e^{-\frac{\nu}{\alpha} l} \right) + i \sin\left(\frac{\mu l}{\alpha}\right) \left(e^{\frac{\nu}{\alpha} l} + e^{-\frac{\nu}{\alpha} l} \right) = 0. \quad (46)$$

This equation is only true if both

$$\cos\left(\frac{\mu l}{\alpha}\right) \left(e^{\frac{\nu}{\alpha} l} - e^{-\frac{\nu}{\alpha} l} \right) = 0 \quad (47)$$

and

$$i \sin\left(\frac{\mu l}{\alpha}\right) \left(e^{\frac{\nu}{\alpha} l} + e^{-\frac{\nu}{\alpha} l} \right) = 0. \quad (48)$$

Since $e^{\frac{\nu}{\alpha} l} + e^{-\frac{\nu}{\alpha} l}$ in equation (48) is always bigger than 0, we can say that

$$i \sin\left(\frac{\mu l}{\alpha}\right) = 0. \quad (49)$$

Dividing by i on both sides yields

$$\sin\left(\frac{\mu l}{\alpha}\right) = 0. \quad (50)$$

For $\sin\left(\frac{\mu l}{\alpha}\right)$ to equal 0, $\frac{\mu l}{\alpha}$ must be a whole multiple of π . Thus

$$\frac{\mu l}{\alpha} = n\pi, \quad n \in \mathbb{N}. \quad (51)$$

By rearranging for μ , we obtain

$$\mu = \frac{n\pi\alpha}{l}. \quad (52)$$

Using this μ in equation (47) gives us

$$\cos(n\pi) \left(e^{\frac{\nu}{\alpha}l} - e^{-\frac{\nu}{\alpha}l} \right) = 0. \quad (53)$$

Since $\cos(n\pi)$ is never 0, we can safely assume that

$$e^{\frac{\nu}{\alpha}l} - e^{-\frac{\nu}{\alpha}l} = 0. \quad (54)$$

Equation (54) is only satisfied for $\nu = 0$. Therefore

$$\lambda = \mu + 0i. \quad (55)$$

Hence

$$\lambda = \mu = \frac{n\pi\alpha}{l}. \quad (56)$$

We now return to equation (33). Substituting in λ , we obtain

$$\alpha^2 X'' + \frac{n^2\pi^2\alpha^2}{l^2} X = 0. \quad (57)$$

By dividing by α^2 on both sides, we find that

$$X'' + \frac{n^2\pi^2}{l^2} X = 0. \quad (58)$$

The simple solution ψ to this ordinary differential equation is of the form

$$\psi(x) = \sin\left(\frac{n\pi x}{l}\right), \quad (59)$$

since substituting equation (59) into equation (58) yields

$$-\frac{n^2\pi^2}{l^2} \cdot \sin\left(\frac{n\pi x}{l}\right) + \frac{n^2\pi^2}{l^2} \cdot \sin\left(\frac{n\pi x}{l}\right) = 0. \quad (60)$$

Since this a true statement, equation (60) is indeed a valid solution of equation (32).

In an identical manner, we can also solve for $Y(y)$. Here we will use m , where $m \in \mathbb{N}$, instead of n to denote the positive integer and h instead of l to denote the height of the plate. Otherwise, $\psi(y)$ is essentially the same as $\psi(x)$:

$$\psi(y) = \sin\left(\frac{m\pi y}{h}\right). \quad (61)$$

In order to solve for $\psi(t)$ we must return to equation (31). Since $\sigma = -\lambda^2$,

$$\sigma = -\frac{n^2\pi^2\alpha^2}{l^2} \quad (62)$$

and similarly,

$$\gamma = -\frac{m^2\pi^2\alpha^2}{h^2}. \quad (63)$$

Substituting γ and σ into equation (31) yields

$$T'' + \left(\frac{n^2\pi^2\alpha^2}{l^2} + \frac{m^2\pi^2\alpha^2}{h^2}\right)T = 0. \quad (64)$$

This ordinary differential equation has the simple solution

$$\psi(t) = \sin\left(t\pi\alpha\sqrt{\frac{n^2}{l^2} + \frac{m^2}{h^2}}\right). \quad (65)$$

Notice that we have to choose sine and not cosine in order to satisfy the boundary conditions (16), (18) and (20).

Finally, since $u(x, y, t) = X(x)Y(y)T(t) = \psi(x)\psi(y)\psi(t)$, we obtain the solution

$$u(x, y, t) = \sin\left(\frac{n\pi x}{l}\right) \sin\left(\frac{m\pi y}{h}\right) \sin\left(t\pi\alpha\sqrt{\frac{n^2}{l^2} + \frac{m^2}{h^2}}\right), \quad (66)$$

where n is the number of nodes in x direction without counting the node at $x = 0$, m is the number of nodes in y direction without counting the node at $y = 0$, l is the length of the plate in x direction and h is the height of the plate in y direction. For a complete description of the physical system, our solution would have to take the form of a linear combination of all particular solutions represented by equation (66). However, since we are only looking for the natural modes of the plate, which are represented by the particular solutions (66), our solution is sufficient for predicting the formation of Chladni figures.

4 Nodes on a Rectangular Plate

4.1 Nodes in the x Direction

As previously discussed, Chladni figures form where $u(x, y, t) = 0$. Since our equation (66) describing the formation of Chladni figures on a rectangular plate is composed of three parts $\psi(x)$, $\psi(y)$ and $\psi(t)$ which are multiplied together, $u(x, y, t)$ will equal 0 when any one of these parts equals 0. We can therefore separate the nodes of each part and look at them individually. We will start with the nodes in the x direction. We are therefore searching for the values for which $\psi(x) = 0$:

$$\psi(x) = \sin\left(\frac{n\pi x}{l}\right) = 0. \quad (67)$$

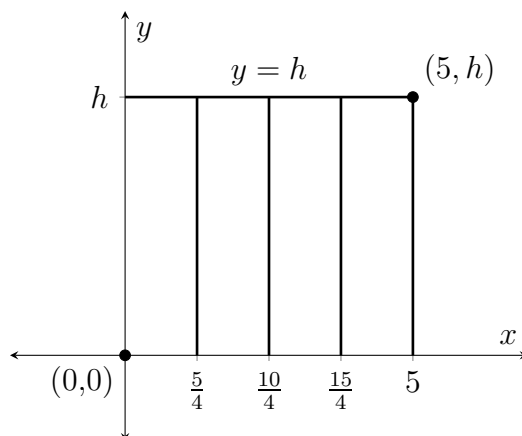
For this equation to be true, $\frac{n\pi x}{l}$ must equal a whole multiple of π . Thus we write

$$\frac{n\pi x}{l} = p_x\pi, \quad p_x \in \mathbb{N}, \quad p_x \leq n. \quad (68)$$

Dividing by π on both sides and rearranging for x yields

$$x = \frac{lp_x}{n}. \quad (69)$$

This tells us that nodes will occur when x is a whole multiple of $\frac{l}{n}$. To illustrate this with an example, we use a plate with the length $l = 5\text{m}$ and we will let $n = 4$:



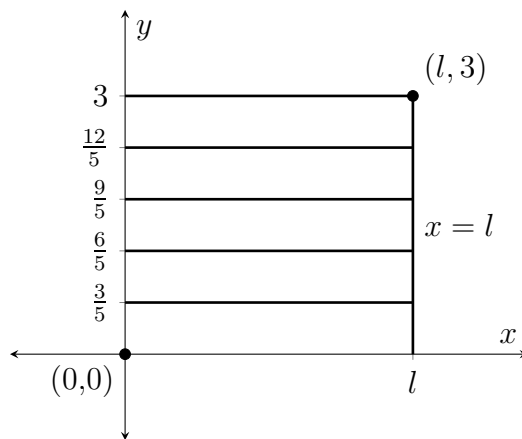
The value p_x in equation (69) is a sort of numerator for the nodes. $p_x = 0$ gives us the node at $x = 0$, $p_x = 1$ gives us the node at $x = \frac{5}{4}\text{m}$ and so on, until $p_x = 4 = n$ gives us the node at $x = 5\text{m}$.

4.2 Nodes in the y Direction

In identical manner to the x coordinate nodes, we can say that the y coordinate nodes will occur when $\psi(y) = 0$. Following the same steps as in the previous subsection gives us y coordinate nodes when

$$y = \frac{hp_y}{m}, \quad p_y \in \mathbb{N}, \quad p_y \leq m. \quad (70)$$

Similar to the x coordinate nodes, y coordinate nodes occur when y is a whole multiple of $\frac{h}{m}$. As an example, we will let $h = 3m$ and $m = 5$:



Note that p_y is again a sort of numerator for the nodes. $p_y = 0$ gives us the node at $y = 0$, $p_y = 1$ gives us the node at $y = \frac{3}{5}m$ and so on, until $p_y = 5 = m$ gives us the node at $y = 3m$.

4.3 Nodes in the t Direction

Despite seeming quite counter-intuitive, in the same way that we can find nodes for the x and y coordinates, there are also nodes for the t -coordinates, where the displacement of the entire plate is 0. Analogously to the x and y nodes, t nodes occur when $\phi(t) = 0$. We can say

$$\sin \left(t\alpha\pi\sqrt{\frac{n^2}{l^2} + \frac{m^2}{h^2}} \right) = 0. \quad (71)$$

Thus

$$t\pi\alpha\sqrt{\frac{n^2}{l^2} + \frac{m^2}{h^2}} = p_t\pi, \quad p_t \in \mathbb{N}. \quad (72)$$

Squaring and dividing by π^2 on both sides yields

$$t^2 \alpha^2 \left(\frac{n^2}{l^2} + \frac{m^2}{h^2} \right) = p_t^2. \quad (73)$$

Rearranging for t^2 gives us

$$t^2 = p_t^2 \frac{l^2 h^2}{n^2 \alpha^2 h^2 + m^2 \alpha^2 l^2}. \quad (74)$$

This then gives us the following expression for t

$$t = p_t \sqrt{\frac{l^2 h^2}{n^2 \alpha^2 h^2 + m^2 \alpha^2 l^2}}. \quad (75)$$

This equation tells us that $\psi(t) = 0$ when t is a whole multiple of $\sqrt{\frac{l^2 h^2}{n^2 \alpha^2 h^2 + m^2 \alpha^2 l^2}}$. Now what does this actually mean for the physical system? If we think of a specific point on the plate with the coordinates (x, y) such that $x \neq \frac{lp_x}{n}$ and $y \neq \frac{hp_y}{m}$, then $u(x, y, t)$ will equal 0 only when t is a multiple of $\sqrt{\frac{l^2 h^2}{n^2 \alpha^2 h^2 + m^2 \alpha^2 l^2}}$. Essentially this expression for which $\psi(t) = 0$ is analogous to half of the period of the function drawn out by the point (x, y) through time. We can therefore say that the period (T) of the oscillation of the plate is

$$T = 2 \sqrt{\frac{l^2 h^2}{n^2 \alpha^2 h^2 + m^2 \alpha^2 l^2}}. \quad (76)$$

Since the frequency of the oscillation (f) is equal to $\frac{1}{T}$ equation (76) takes the form

$$f = \frac{\alpha}{2lh} \sqrt{n^2 h^2 + m^2 l^2}. \quad (77)$$

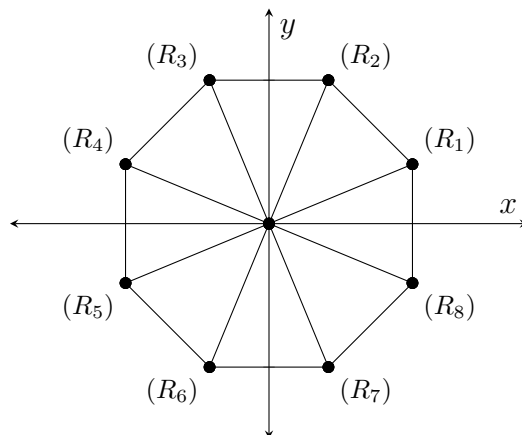
This tells us that for a specific choice of the positive integers n and m , the propagation speed of the wave α and the length l and height h of the plate, there is a specific frequency at which the Chladni figures will form, as represented by equation (77).

5 Chladni Figures on a Circular Plate

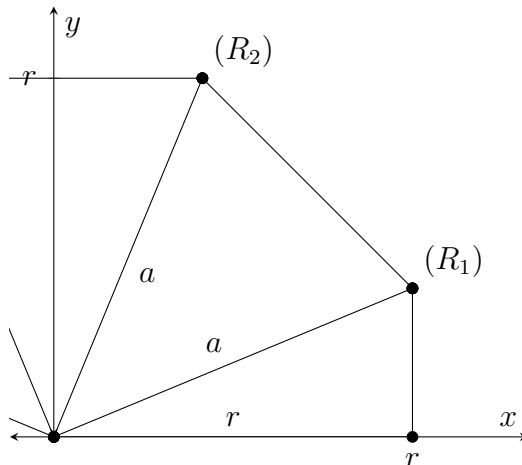
5.1 Boundary Conditions for a Circular Plate

In order to solve the wave equation for a circular plate we have the elegant solution of converting the wave equation into polar coordinates and solving it accordingly. However in this section, we will solve the wave equation for a circular plate by approximating a circle with polygons in the regular Cartesian coordinate system. We shall later compare our solutions with those of the polar wave equation.

We will only work with polygons with 2^n sides to keep symmetry amongst all quadrants. We will also define the point $(0,0)$ as the center of each polygon. To illustrate how we will proceed, we shall use the example of a 2^3 -gon also known as an octagon.



We shall now only focus on the first quadrant of the octagon.



We now wish to describe the position of the corner-points of the polygon in dependence of the bisector r and the amount of corners the 2^n -gon has, which is dependent on n . First we will describe the angle θ $(R_1, 0, x)$ using n . Since 360° is equivalent to 2π radians, we can say that 2θ times the amount of polygons, 2^n , is equal to one entire rotation:

$$2\theta \cdot 2^n = 2\pi. \quad (78)$$

By dividing by 2^n , we obtain

$$2\theta = \frac{2\pi}{2^n}. \quad (79)$$

This gives the following expression for θ :

$$\theta = \frac{\pi}{2^n}. \quad (80)$$

Now we describe the distance a using r and $\theta = \frac{\pi}{2^n}$. Since $\cos(\theta)$ is defined as $\frac{r}{a}$, we can describe the legs of the triangle, a , in the following way:

$$a = \frac{r}{\cos(\theta)} = \frac{r}{\cos(\frac{\pi}{2^n})}. \quad (81)$$

We now wish to find the coordinates (R_{kx}, R_{ky}) of each point R_k . Noticing that the length a is the radial distance between $(0,0)$ and the point R_k , we can divide a into its vertical and horizontal components R_{kx} and R_{ky} . These values are a function of the counterclockwise angle between the x axis and a . Since we have the angle $1 \cdot \theta$ for $k = 1$, $3 \cdot \theta$ for $k = 2$, ect., this angle $(R_k, 0, x)$ will always be a odd multiple of θ . We therefore write $(2k - 1)\theta$ to denote this angle. This is also the reason that we count R_k in the counterclockwise direction starting from the closest point to the x axis in the first quadrant.

$$R_{kx} = \cos\left((2k - 1)\theta\right) \cdot a, \quad (82)$$

$$R_{ky} = \sin\left((2k - 1)\theta\right) \cdot a. \quad (83)$$

We now insert θ from equation (79) and a from equation (81). It follows that

$$R_{kx} = \cos\left((2k - 1)\frac{\pi}{2^n}\right) \cdot \frac{r}{\cos(\frac{\pi}{2^n})}, \quad (84)$$

$$R_{ky} = \sin\left((2k - 1)\frac{\pi}{2^n}\right) \cdot \frac{r}{\cos(\frac{\pi}{2^n})}. \quad (85)$$

As such, each vertex of the polygon R_k can be described by the coordinate

$$R_k = \left(\cos\left((2k - 1)\frac{\pi}{2^n}\right) \cdot \frac{r}{\cos(\frac{\pi}{2^n})}, \sin\left((2k - 1)\frac{\pi}{2^n}\right) \cdot \frac{r}{\cos(\frac{\pi}{2^n})} \right). \quad (86)$$

For simplicity, we will refer to these coordinates as R_{kx} and R_{ky} respectively in future calculations.

5.2 Solving the Wave Equation for a Circular Plate

To find fitting boundary conditions for the polygon approximation method, we shall consider only the legs of the triangles in our polygon. These lines can be considered to be fine strips, which trace out the shape of the polygon and the radial lines connecting $(0, 0)$ with each corner. Knowing that each corner and the center of the polygon are fixed, we can set up the following boundary conditions for these thin strips:

$$u(R_{kx}, y, t) = 0, \quad (87)$$

$$u(x, R_{ky}, t) = 0, \quad (88)$$

$$u(0, y, t) = 0, \quad (89)$$

$$u(x, 0, t) = 0. \quad (90)$$

We also set the initial displacement to be 0:

$$u(x, y, 0) = 0. \quad (91)$$

Using these boundary conditions, we can solve the wave equation for fine strips in two dimensions. Analogous to the procedure shown in section 3, we can separate $u(x, y, t)$ into $X(x)Y(y)T(t)$. Following the same derivation as for equation (38), we can start directly from the general solution of $X(x)$

$$\phi(x) = c_1 e^{\frac{i\lambda}{\alpha}x} + c_2 e^{-\frac{i\lambda}{\alpha}x}. \quad (92)$$

Applying the boundary condition (89) we can say

$$c_1 + c_2 = 0. \quad (93)$$

Similarly, by using the boundary condition (87) on equation (92), we obtain

$$\phi(l) = c_1 e^{\frac{i\lambda}{\alpha}l} + c_2 e^{-\frac{i\lambda}{\alpha}l} = 0. \quad (94)$$

Similar to equation (42), this equation is valid for $c_1 = c_2 = 0$. However using these constants would result in $u(x, y, t) = 0$ at all times for any x and y , which we can clearly see is not the case for the physical system, since Chladni figures would not form. Moreover, since $c_1 = -c_2$, neither c_1 nor c_2 are allowed to be 0. This is only the case if

$$e^{\frac{i\lambda R_{kx}}{\alpha}} - e^{-\frac{i\lambda R_{kx}}{\alpha}} = 0. \quad (95)$$

We can see the similarities between equation (95) and equation (43) hence it is no surprise that the solution to this equation is very similar to that derived in section 3. Following the same process as in section 3 we find the following solution for $X(x)$:

$$\psi(x) = \sin\left(\frac{g\pi x}{R_{kx}}\right), \quad g \in \mathbb{N} \quad (96)$$

We can also solve for $Y(y)$ in an identical manner. Unlike section three, we also use g to denote the positive integer for $\psi(y)$ because the plate is fully symmetrical. Therefore the number of nodes in the y direction is the same as in the x direction. We also use the coordinate R_{ky} since we are looking at the y component of the equation. Otherwise, $\psi(y)$ is essentially the same as $\psi(x)$:

$$\psi(y) = \sin\left(\frac{g\pi y}{R_{ky}}\right). \quad (97)$$

Using the same method as in section three, we also obtain the following solution for $T(t)$:

$$\psi(t) = \sin\left(t\pi\alpha\sqrt{\frac{g^2}{R_{kx}^2} + \frac{g^2}{R_{ky}^2}}\right). \quad (98)$$

We can very clearly see in the equation above how the solution implies symmetrical x and y nodes, since we only have one positive integer g . We hence have the following expression for $T(t)$:

$$\psi(t) = \sin\left(tg\pi\alpha\sqrt{\frac{1}{R_{kx}^2} + \frac{1}{R_{ky}^2}}\right). \quad (99)$$

This leads to the solution

$$u_k(x, y, t) = \sin\left(\frac{g\pi x}{R_{kx}}\right) \sin\left(\frac{g\pi y}{R_{ky}}\right) \sin\left(tg\pi\alpha\sqrt{\frac{1}{R_{kx}^2} + \frac{1}{R_{ky}^2}}\right). \quad (100)$$

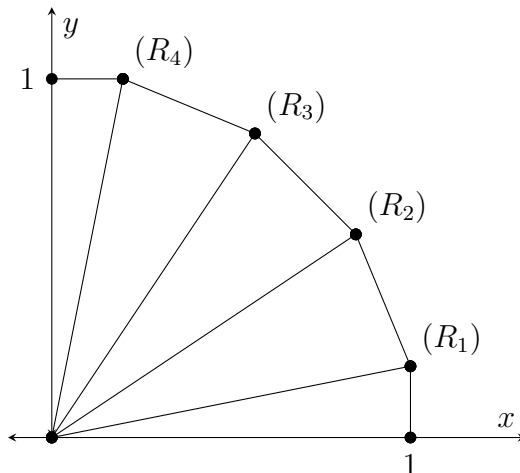
Substituting R_{kx} and R_{ky} from equations (84) and (85) gives us the following system of solutions:

$$u_k(x, y, t) = \sin\left(\frac{g\pi x}{\cos\left((2k-1)\frac{\pi}{2^n}\right) \cdot \frac{r}{\cos\left(\frac{\pi}{2^n}\right)}\right) \sin\left(\frac{g\pi y}{\sin\left((2k-1)\frac{\pi}{2^n}\right) \cdot \frac{r}{\cos\left(\frac{\pi}{2^n}\right)}\right) \cdot \sin\left(tg\pi\alpha\sqrt{\frac{1}{\left[\cos\left((2k-1)\frac{\pi}{2^n}\right) \cdot \frac{r}{\cos\left(\frac{\pi}{2^n}\right)}\right]^2} + \frac{1}{\left[\sin\left((2k-1)\frac{\pi}{2^n}\right) \cdot \frac{r}{\cos\left(\frac{\pi}{2^n}\right)}\right]^2}}\right). \quad (101)$$

This equation describes the behaviour of each individual radial strip. Depending on what values n and r will take, each strip between $(0,0)$ and the points R_k ends up having a different equation, depending on k , which describes it. As we go to an infinite polygon, the strips get closer and closer together, to become one continuous plate when the polygon becomes a circle. We do not obtain an analytical solution for the formation of the chladni figures. However by plotting the values for very big polygons, we can get quite close to having the same output as an analytical solution for a circular plate. Unfortunately, analytical solutions in cylindrical coordinates do not involve regular sinusoid functions, which implies, that the nodes would not be evenly spaced between the center and edge of the plate. We shall discuss the cylindrical wave equation in sections 6 and 7.

5.3 Nodes on a Circular Plate

Solving for the nodes on a circular plate is essentially the same as on a rectangular plate. We can interpret the solution (101) as the wave equation for 2^n different rectangles, whose edges are R_{kx} and R_{ky} . We do however only consider the strip joining $(0,0)$ and (R_{kx}, R_{ky}) , since this is what the boundary conditions take into account. We shall look at the first quadrant of the example: $n = 4$, $r = 1\text{m}$ and $g = 3$.



For the arbitrarily chosen $k = 3$, the boundary conditions used in section 5.2 would, in theory, solve the wave equation for a rectangular plate of the dimensions R_{3x} by R_{3y} . Remember however, that we chose only to define the fine strip spanning from the origin to (R_3) , since this is the situation for which these boundary conditions are actually valid for the physical system.

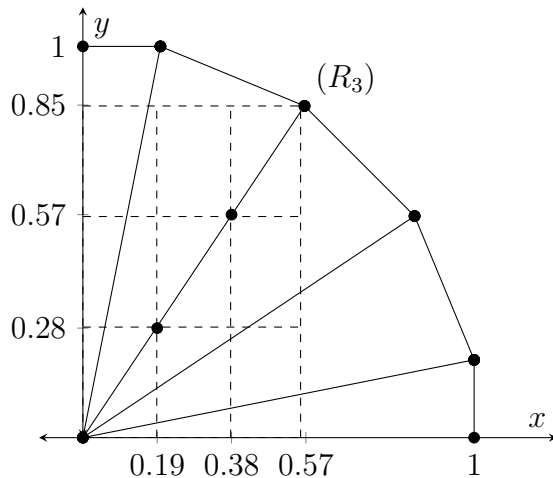
Solving for the nodes in the same manner as in section 4 yields that x-nodes form when

$$x = \frac{R_{kx}p}{g}, \quad p \in \mathbb{N}, \quad p \leq g \quad (102)$$

and y-nodes form when

$$y = \frac{R_{ky}p}{g}, \quad p \in \mathbb{N}, \quad p \leq g. \quad (103)$$

Notice again that the same positive integer g is used for both descriptions of the nodal patterns, since we cannot have a different number of x and y nodes. We now return to the previous example of $n = 4$, $r = 1\text{m}$ and $g = 3$. We now choose $k = 3$. According to equations (102) and (103), this will give us nodes at $x \approx 0\text{m}, 0.19\text{m}, 0.38\text{m}, 0.57\text{m}$ and $y \approx 0\text{m}, 0.28\text{m}, 0.57\text{m}, 0.85\text{m}$.



This now gives us the following points for which $u(x, y, t) = 0$: $(0, 0)$, $(0.19, 0.28)$, $(0.38, 0.57)$ and $R_3 \approx (0.57, 0.85)$. Doing this for all R_k for bigger and bigger polygons results in these points slowly forming continuous concentric circles around the origin. As n goes to infinity the radii of these circles approach $\frac{rp}{g}$.

5.4 t - Nodes on a Circular Plate

Since $\psi(t)$ differs slightly from equation (65) for the circular plate, we shall more rigorously discuss at the nodes as a function time. We begin as in section 3:

$$\psi(t) = \sin \left(tg\pi\alpha \sqrt{\frac{1}{R_{kx}^2} + \frac{1}{R_{ky}^2}} \right) = 0. \quad (104)$$

For $\psi(t) = 0$ the contents of the sine function must be equal to a whole multiple of π . We write

$$tg\pi\alpha\sqrt{\frac{1}{R_{kx}^2} + \frac{1}{R_{ky}^2}} = p_t\pi, \quad p_t \in \mathbb{N}. \quad (105)$$

Dividing by π on both sides and rearranging for t yields:

$$t = \frac{p_t}{g\alpha\sqrt{\frac{1}{R_{kx}^2} + \frac{1}{R_{ky}^2}}}, \quad (106)$$

which we can also write as:

$$t = \frac{p_t R_{kx} R_{ky}}{g\alpha\sqrt{R_{kx}^2 + R_{ky}^2}}. \quad (107)$$

Inserting the full values for R_{kx} and R_{ky} gives us

$$t = \frac{p_t \cos\left((2k-1)\frac{\pi}{2^n}\right) \cdot \frac{r}{\cos\left(\frac{\pi}{2^n}\right)} \sin\left((2k-1)\frac{\pi}{2^n}\right) \cdot \frac{r}{\cos\left(\frac{\pi}{2^n}\right)}}{g\alpha\sqrt{\left[\cos\left((2k-1)\frac{\pi}{2^n}\right) \cdot \frac{r}{\cos\left(\frac{\pi}{2^n}\right)}\right]^2 + \left[\sin\left((2k-1)\frac{\pi}{2^n}\right) \cdot \frac{r}{\cos\left(\frac{\pi}{2^n}\right)}\right]^2}} \quad (108)$$

Similarly to section 4, the reciprocal of this equation should tell us the frequency at which the plate would have to vibrate in order to create the radial nodes on our thin strip. Unfortunately each plate has a different side length (R_{kx}) and height (R_{ky}), which gives us different frequencies for each string. This does not make logical sense, since they theoretically all have the same initial conditions, length and constant α . Since a circle is formed as the number of vertices in the 2^n -gon goes to infinity, we would like to let n go to infinity in equation (108). When we let n go to infinity, four strips will be vibrating along the x and y axes. This results in (R_{kx}) or (R_{ky}) respectively to become zero. This effectively results in all the x or y nodes to be compressed down to one single node, along the corresponding axis. For this to occur, the frequency of the vibration would have to be infinitely large. Therefore our solution does not apply for $\psi(t)$. Thus, equation (101) is incomplete and does not fully describe the physical system. To get an appropriate solution which can also predict the frequency at which the patterns form, we have to solve the one dimensional wave equation for a string fixed at $x = 0$ and $x = \sqrt{R_{kx}^2 + R_{ky}^2}$. We begin with the one dimensional wave equation:

$$\frac{\partial^2 u}{\partial t^2} = \alpha^2 \frac{\partial^2 u}{\partial x^2}, \quad (109)$$

where we have the following boundary conditions:

$$u(0, t) = 0, \quad (110)$$

$$u\left(\sqrt{R_{kx}^2 + R_{ky}^2}, t\right) = 0, \quad (111)$$

$$u(x, 0) = 0. \quad (112)$$

To solve equation (109) we will again use the separation of variables technique. We assume that $u(x, t)$ can be expressed as the product of two functions $X(x)$ and $T(t)$ which are both only dependent on one unique variable. We will write $T(t)$ as T and $X(x)$ as X . The one dimensional wave equation becomes

$$T''X = \alpha^2TX''. \quad (113)$$

Dividing by T and X on both sides gives us

$$\frac{T''}{T} = \alpha^2\frac{X''}{X}. \quad (114)$$

Analogously to section 3 and since both sides of this equation are equal, each side must be equal to the same constant, which we will again call σ . We find two ordinary differential equations:

$$\frac{T''}{T} = \sigma, \quad (115)$$

$$\alpha^2\frac{X''}{X} = \sigma. \quad (116)$$

Since equation (116) is identical to equation (27) it comes as no surprise that they share the same general solution

$$\phi(x) = c_1e^{\frac{i\lambda}{\alpha}x} + c_2e^{-\frac{i\lambda}{\alpha}x}. \quad (117)$$

Again in similar fashion to section 3, we use the boundary condition (110) on equation (117). It follows that

$$c_1 + c_2 = 0. \quad (118)$$

Subsequently, applying boundary condition (111) results in

$$\phi\left(\sqrt{R_{kx}^2 + R_{ky}^2}\right) = c_1e^{\frac{i\lambda\sqrt{R_{kx}^2 + R_{ky}^2}}{\alpha}} + c_2e^{-\frac{i\lambda\sqrt{R_{kx}^2 + R_{ky}^2}}{\alpha}} = 0. \quad (119)$$

To avoid clutter, we will write $\sqrt{R_{kx}^2 + R_{ky}^2}$ as δ . Then

$$\phi(\delta) = c_1 e^{\frac{i\lambda\delta}{\alpha}} + c_2 e^{-\frac{i\lambda\delta}{\alpha}} = 0. \quad (120)$$

Notice that equation (120) is essentially the same as equation (42). As such, it is not surprising that their solution is also very similar. The only difference is that l has become δ . We find that

$$\psi(x) = \sin\left(\frac{g\pi x}{\delta}\right) = 0, \quad g \in \mathbb{N}. \quad (121)$$

We also obtain $\sigma = -\frac{n^2\pi^2\alpha^2}{\delta^2}$ analogously to equation (62). We can insert σ into equation (115). Hence

$$\frac{T''}{T} = -\frac{g^2\pi^2\alpha^2}{\delta^2}. \quad (122)$$

Thus

$$T'' + \frac{g^2\pi^2\alpha^2}{\delta^2}T = 0. \quad (123)$$

This ordinary differential equation has the simple solution

$$\psi(t) = \sin\left(\frac{g\pi\alpha t}{\delta}\right). \quad (124)$$

To obtain a more complete solution for our physical system we can now replace $\psi(t)$ in equation (100) with equation (124). We have

$$u(x, y, t) = \sin\left(\frac{g\pi x}{R_{kx}}\right) \sin\left(\frac{g\pi y}{R_{ky}}\right) \sin\left(\frac{g\pi\alpha t}{\delta}\right). \quad (125)$$

Finally, by inserting the full values for δ , R_{kx} and R_{ky} , we find that our solution for the circular plate is now of the form

$$u(x, y, t) = \sin\left(\frac{g\pi x}{\cos\left((2k-1)\frac{\pi}{2^n}\right) \cdot \frac{r}{\cos\left(\frac{\pi}{2^n}\right)}}\right) \sin\left(\frac{g\pi y}{\sin\left((2k-1)\frac{\pi}{2^n}\right) \cdot \frac{r}{\cos\left(\frac{\pi}{2^n}\right)}}\right) \cdot \sin\left(\frac{g\pi\alpha t}{\sqrt{\left(\cos\left((2k-1)\frac{\pi}{2^n}\right) \cdot \frac{r}{\cos\left(\frac{\pi}{2^n}\right)}\right)^2 + \left(\sin\left((2k-1)\frac{\pi}{2^n}\right) \cdot \frac{r}{\cos\left(\frac{\pi}{2^n}\right)}\right)^2}}\right). \quad (126)$$

This is a hybrid of a one dimensional and two dimensional solution, which gives the placement of the nodes as well as the frequency at which they occur. This can be calculated by letting the new $\psi(t)$ equal 0. Thus, the argument of the sine function must be a whole multiple of π . We write

$$\frac{g\pi\alpha t}{\sqrt{R_{kx}^2 + R_{ky}^2}} = p_t\pi, \quad p_t \in \mathbb{N}. \quad (127)$$

Dividing by π and rearranging for t yields

$$t = \frac{p_t \sqrt{R_{kx}^2 + R_{ky}^2}}{g\alpha}. \quad (128)$$

As in section 4.3, this equation gives us the following period T :

$$T = 2 \frac{\sqrt{R_{kx}^2 + R_{ky}^2}}{g\alpha}. \quad (129)$$

Thus, the frequency at which the Chladni figures form is

$$f = \frac{g\alpha}{2\sqrt{R_{kx}^2 + R_{ky}^2}}. \quad (130)$$

As we let n go to infinity, the 2^n -gon approaches a circle. In this case $\sqrt{R_{kx}^2 + R_{ky}^2}$ becomes r . Therefore the frequency at which the Chladni figures form for a circular plate would be

$$f = \frac{g\alpha}{2\sqrt{R_{kx}^2 + R_{ky}^2}} = \frac{g\alpha}{2r}. \quad (131)$$

6 Polar Form of the Two Dimensional Wave Equation

The more common method for solving the wave equation for a circular plate is to first convert the wave equation into its polar form.

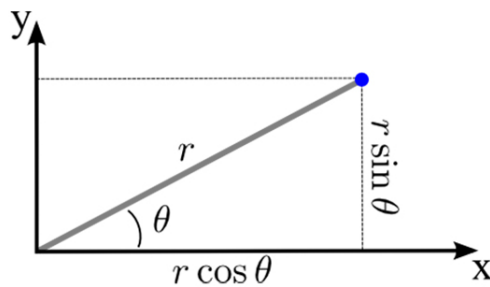


Figure 5: Correlation between Cartesian and Polar coordinates [5]

We begin with the normal wave equation in cartesian coordinates:

$$\frac{1}{\alpha^2} \frac{\partial^2 u}{\partial t^2} = \frac{\partial^2 u}{\partial x^2} + \frac{\partial^2 u}{\partial y^2}. \quad (132)$$

We now wish to replace the function $u(x, y, t)$ by it's polar counterpart $u(r, \theta, t)$, where

$$r = \sqrt{x^2 + y^2}, \quad (133)$$

$$\theta = \arctan\left(\frac{y}{x}\right), \quad (134)$$

$$\frac{x}{r} = \cos(\theta), \quad (135)$$

$$\frac{y}{r} = \sin(\theta). \quad (136)$$

Since we know that $\frac{\partial u}{\partial r}$ depends on x and y , we can use the chain rule in Leibniz notation [7] to write

$$\frac{\partial u}{\partial r} = \frac{\partial u}{\partial x} \frac{\partial x}{\partial r} + \frac{\partial u}{\partial y} \frac{\partial y}{\partial r}. \quad (137)$$

Using equations (135) and (136) we find that

$$\frac{\partial u}{\partial r} = \frac{\partial u}{\partial x} \cos(\theta) + \frac{\partial u}{\partial y} \sin(\theta). \quad (138)$$

We can also write $\frac{\partial u}{\partial \theta}$ in the same way using the chain rule:

$$\frac{\partial u}{\partial \theta} = \frac{\partial u}{\partial x} \frac{\partial x}{\partial \theta} + \frac{\partial u}{\partial y} \frac{\partial y}{\partial \theta}. \quad (139)$$

We also know that

$$\frac{\partial x}{\partial \theta} = \frac{\partial(r \cos(\theta))}{\partial \theta} = -r \sin(\theta) \quad (140)$$

and

$$\frac{\partial y}{\partial \theta} = \frac{\partial(r \sin(\theta))}{\partial \theta} = r \cos(\theta). \quad (141)$$

As such, equation (139) takes the form

$$\frac{\partial u}{\partial \theta} = \frac{\partial u}{\partial x} (-r \sin(\theta)) + \frac{\partial u}{\partial y} r \cos(\theta). \quad (142)$$

We shall now use the following notation to denote partial derivatives:

$$\frac{\partial u}{\partial x} = u_x, \quad (143)$$

$$\frac{\partial u}{\partial y} = u_y, \quad (144)$$

$$\frac{\partial u}{\partial r} = u_r, \quad (145)$$

$$\frac{\partial u}{\partial \theta} = u_\theta. \quad (146)$$

Solving equations (138) and (142) for u_x yields the following system of equations:

$$u_x = \frac{u_r - u_y \sin(\theta)}{\cos(\theta)} \quad (147)$$

and

$$u_x = \frac{u_\theta - u_y r \cos(\theta)}{-r \sin(\theta)}. \quad (148)$$

Since the right side of these two equations are both equal to u_x , they must consequentially also be equal to each other. We obtain

$$\frac{u_\theta - u_y r \cos(\theta)}{-r \sin(\theta)} = \frac{u_r - u_y \sin(\theta)}{\cos(\theta)}. \quad (149)$$

Rearranging for u_y gives us

$$\frac{u_r \sin(\theta)}{\sin^2 \theta + \cos^2 \theta} + \frac{1}{r} \frac{u_\theta \cos(\theta)}{\sin^2 \theta + \cos^2 \theta} = u_y. \quad (150)$$

Since $\sin^2 \theta + \cos^2 \theta = 1$, equation (150) becomes

$$u_y = u_r \sin(\theta) + \frac{1}{r} u_\theta \cos(\theta). \quad (151)$$

We now insert this equation into equation (148). We find that

$$u_x = u_r \cos(\theta) - \frac{1}{r} u_\theta \sin(\theta). \quad (152)$$

Using the chain rule again, we can now write the second derivatives in the following way:

$$u_{xx} = \frac{\partial u_x}{\partial r} \frac{\partial r}{\partial x} + \frac{\partial u_x}{\partial \theta} \frac{\partial \theta}{\partial x}. \quad (153)$$

Observe the relation

$$\frac{\partial \theta}{\partial x} = \frac{\partial \arctan(\frac{y}{x})}{\partial x} = -\frac{y}{r^2} = -\frac{\sin(\theta)}{r}. \quad (154)$$

Similarly,

$$\frac{\partial \theta}{\partial y} = \frac{\cos(\theta)}{r}. \quad (155)$$

We can also rewrite $\frac{\partial r}{\partial x}$ and $\frac{\partial r}{\partial y}$ as

$$\frac{\partial r}{\partial x} = \cos(\theta), \quad (156)$$

$$\frac{\partial r}{\partial y} = \sin \theta. \quad (157)$$

Using the relations above and equation (152), equation (154) takes the form

$$u_{xx} = \frac{\partial(u_r \cos(\theta) - \frac{1}{r} u_\theta \sin(\theta))}{\partial r} \cos(\theta) - \frac{\partial(u_r \cos(\theta) - \frac{1}{r} u_\theta \sin(\theta))}{\partial \theta} \frac{\sin(\theta)}{r}. \quad (158)$$

Taking the derivatives with respect to r and θ and expanding yields

$$u_{xx} = u_{rr} \cos^2 \theta - \frac{2}{r} u_{r\theta} \sin(\theta) \cos(\theta) + \frac{2}{r^2} u_{\theta\theta} \sin(\theta) \cos(\theta) + \frac{1}{r} u_r \sin^2 \theta + \frac{1}{r^2} u_{\theta\theta} \sin^2 \theta. \quad (159)$$

Similarly, u_{yy} is given by

$$u_{yy} = u_{rr} \sin^2 \theta + \frac{2}{r} u_{r\theta} \sin(\theta) \cos(\theta) - \frac{2}{r^2} u_{\theta\theta} \sin(\theta) \cos(\theta) + \frac{1}{r} u_r \cos^2 \theta + \frac{1}{r^2} u_{\theta\theta} \cos^2 \theta. \quad (160)$$

We now introduce the Laplace operator in two dimensions ∇^2 , which is defined as

$$\nabla^2 = u_{xx} + u_{yy}. \quad (161)$$

We can insert equations (159) and (160) into the Laplace operator. We find that

$$\begin{aligned} \nabla^2 &= u_{rr} \cos^2 \theta - \frac{2}{r} u_{r\theta} \sin(\theta) \cos(\theta) + \frac{2}{r^2} u_{\theta\theta} \sin(\theta) \cos(\theta) + \frac{1}{r} u_r \sin^2 \theta + \frac{1}{r^2} u_{\theta\theta} \sin^2 \theta \\ &+ u_{rr} \sin^2 \theta + \frac{2}{r} u_{r\theta} \sin(\theta) \cos(\theta) - \frac{2}{r^2} u_{\theta\theta} \sin(\theta) \cos(\theta) + \frac{1}{r} u_r \cos^2 \theta + \frac{1}{r^2} u_{\theta\theta} \cos^2 \theta. \end{aligned} \quad (162)$$

This simplifies down to

$$\nabla^2 = u_{rr} (\cos^2 \theta + \sin^2 \theta) + \frac{1}{r} u_r (\cos^2 \theta + \sin^2 \theta) + \frac{1}{r^2} u_{\theta\theta} (\cos^2 \theta + \sin^2 \theta). \quad (163)$$

Again using $\cos^2 \theta + \sin^2 \theta = 1$, we can write

$$\nabla^2 = u_{rr} + \frac{1}{r} u_r + \frac{1}{r^2} u_{\theta\theta}. \quad (164)$$

Inserting this into the wave equation yields

$$u_{tt} = \alpha^2 \left(u_{rr} + \frac{1}{r} u_r + \frac{1}{r^2} u_{\theta\theta} \right) \quad (165)$$

or

$$\frac{\partial^2 u}{\partial t^2} = \alpha^2 \left(\frac{\partial^2 u}{\partial r^2} + \frac{1}{r} \frac{\partial u}{\partial r} + \frac{1}{r^2} \frac{\partial^2 u}{\partial \theta^2} \right). \quad (166)$$

We have now obtained the wave equation in polar coordinates. A solution method shall be shown in the following section.

7 Application of the Polar Wave Equation on a Circular Plate

We have briefly mentioned the incompleteness of our approximated solution for a circular plate at the end of section 5. We now wish to show the inaccuracy of our approximated solution mathematically. We begin with the polar wave equation:

$$\frac{\partial^2 u}{\partial t^2} = \alpha^2 \left(\frac{\partial^2 u}{\partial r^2} + \frac{1}{r} \frac{\partial u}{\partial r} + \frac{1}{r^2} \frac{\partial^2 u}{\partial \theta^2} \right). \quad (167)$$

Where $u(r, \theta, t)$ is a function of the radius r , the angle θ and time t . To disprove section 5, it suffices to consider only the radially symmetrical solutions. We can therefore discard the part of the equation that is dependent on θ . The wave equation becomes

$$\frac{\partial^2 u}{\partial t^2} = \alpha^2 \left(\frac{\partial^2 u}{\partial r^2} + \frac{1}{r} \frac{\partial u}{\partial r} \right). \quad (168)$$

Analogously to section 3.2, we shall now separate the variables by assuming that $u(r, t)$ can be written as two separate functions: $R(r)T(t)$. We shall write $R(r)$ as R and $T(t)$ as T . It follows that

$$\frac{1}{\alpha^2} RT'' = R''T + \frac{1}{r} R'T. \quad (169)$$

By rearranging terms, we can write:

$$\frac{1}{\alpha^2} \frac{T''}{T} = \frac{R''}{R} + \frac{1}{r} \frac{R'}{R}. \quad (170)$$

Since both sides depend only on one unique variable, we can say that both sides are equal to the same constant, which we shall call $-\lambda^2$. We obtain the following two ordinary differential equations:

$$T'' + T\lambda^2\alpha^2 = 0 \quad (171)$$

and

$$R'' + \frac{1}{r}R' + \lambda^2R = 0. \quad (172)$$

Equation (171) is an equation which we have already seen in the previous sections: its solutions are sinusoids, which are not further interesting for our proof. Equation (172) however is not solvable analytically. We will

therefore write our solution in the form of an infinite polynomial series around $r = 0$. To solve this equation, we will be somewhat following the Frobenius method, since our function is not defined at $r = 0$ due to the term $\frac{1}{r}$. A normal series solution would therefore not be fitting. Now, let us assume, that the solution of equation (172), takes the form

$$R(r) = \sum_{k=0}^{\infty} a_k \cdot r^{k+g}, \quad k \in \mathbb{N}, \quad g \in \mathbb{N}. \quad (173)$$

In this equation, k and g are positive integers. We obtain an infinite polynomial describing our solution. We must now establish the first two derivatives of this function:

$$R'(r) = \sum_{k=0}^{\infty} (k+g)a_k \cdot r^{k+g-1}, \quad (174)$$

$$R''(r) = \sum_{k=0}^{\infty} (k+g-1)(k+g)a_k \cdot r^{k+g-2}. \quad (175)$$

We can now insert these derivatives into equation (172):

$$\sum_{k=0}^{\infty} (k+g-1)(k+g)a_k \cdot r^{k+g-2} + \sum_{k=0}^{\infty} (k+g)a_k \cdot r^{k+g-2} + \lambda^2 \sum_{k=0}^{\infty} a_k \cdot r^{k+g} = 0. \quad (176)$$

This can be rewritten and shortened to the form

$$\sum_{k=0}^{\infty} (k+g-1)(k+g)a_k \cdot r^{k-2} + \sum_{k=0}^{\infty} (k+g)a_k \cdot r^{k-2} + \lambda^2 \sum_{k=2}^{\infty} a_{k-2} \cdot r^{k-2} = 0. \quad (177)$$

Now by calculating the values for $k = 0$ and $k = 1$ it follows that

$$0 = ((g-1)g+g)a_0 r^{-2} + ((g+1)g+g+1)a_1 r^{-1} + \sum_{k=2}^{\infty} [(k+g-1)(k+g) + k+g]a_k + \lambda^2 a_{k-2} r^{k-2}. \quad (178)$$

For this to be true, each of these terms must separately be 0. We obtain the following equation:

$$a_0 r^{-2} ((g-1)g+g) = 0, \quad (179)$$

which yields that $g = 0$. This in turn tells us that a_1 must also equal 0. Inserting our new knowledge into the last part of equation (178) yields the following equation:

$$((k-1) + k)a_k + \lambda^2 a_{k-2} = 0, \quad (180)$$

which becomes

$$k^2 a_k + \lambda^2 a_{k-2} = 0. \quad (181)$$

Thus we find the following recursive condition for our series:

$$a_k = -a_{k-2} \frac{\lambda^2}{k^2}. \quad (182)$$

Now we will let $a_0 = 1$, since stretching and moving the function does not have an effect on its general nature, and plot the first few terms.

$$a_2 = -\frac{\lambda^2}{2^2},$$

$$a_4 = +\frac{\lambda^4}{2^2 \cdot 4^2},$$

$$a_6 = -\frac{\lambda^6}{2^2 \cdot 4^2 \cdot 6^2}.$$

We can write this recurring pattern as

$$a_k = \frac{\lambda^{2k} (-1)^k}{\prod_{j=1}^k (2j)^2}.$$

Since $\prod_{j=1}^k (2j)^2 = (2^k \cdot k!)^2$, our solution to equation (172) is of the form

$$R(r) = \sum_{k=0}^{\infty} \frac{(-1)^k}{(2^k \cdot k!)^2} (r\lambda^2)^k. \quad (183)$$

We still need to make a small adjustment in order to fulfill the boundary condition $R(0) = 0$:

$$R(r) = \sum_{k=0}^{\infty} \frac{(-1)^k}{(2^k \cdot k!)^2} ((r + Q_1)\lambda^2)^k, \quad (184)$$

where Q_1 is the first root of the function. It lies at approximately 5.783 for $\lambda = 1$. If we graph this function we obtain the following wave:

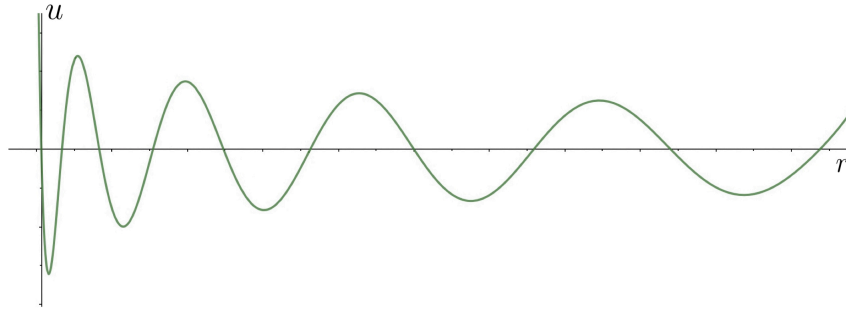


Figure 6: Graph of equation (184) (x -axis: radius r , y -axis: displacement u)

While equation (184) is certainly not a complete solution to the polar wave equation, it sufficiently demonstrates that the roots of the equation are not evenly spaced between the center and edge of the plate. It then follows that the Chladni figures would not be evenly spaced concentric circles. The nodes would be more densely packed toward the center of the plate and less dense toward the rim. Thus our model from section 4, which considered the plate to be an infinite agglomeration of strings, has been shown to be imprecise.

8 Lessons from the Mathematics

As seen in the previous sections, the mathematics describing the nodal figures of Chladni patterns are quite complex. Even simple shapes, such as circles, do not have fully analytical solutions. However, our calculations still predict some interesting behaviors of the plate. On the rectangular membrane, the patterns we obtain are n by m grids. It is surprising, given the intricate nature of Chladni figures, that one would obtain such simple and symmetrical patterns. When we know the solution, however, it intuitively makes sense that a membrane would vibrate in such a way.

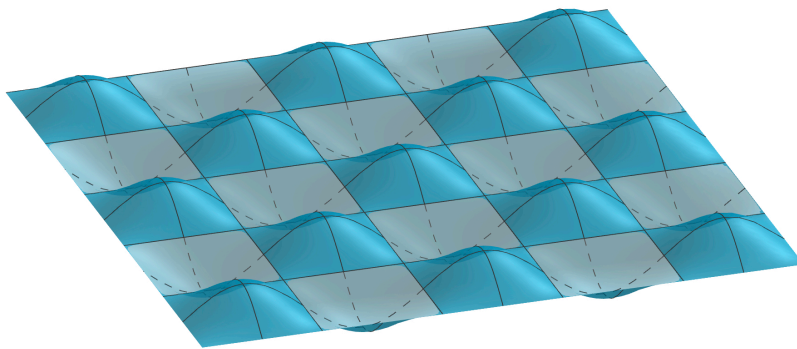


Figure 7: Graph given by equation (66), $n = m = 5$

For the figure 7, we must remember that the system moves over time. Therefore, it is necessary to imagine the oscillation of each rectangle in the grid through time to fully visualize equation (66).

Similarly, when we observe the frequencies at which the figures form (77) as m and n step through integer values, the points gather on the plane depicted by the three dimensional function:

$$f(n, m) = \frac{\alpha}{2lh} \sqrt{n^2 h^2 + m^2 l^2} \quad (185)$$

As we will observe below, we see a linear and symmetrical behavior of the rectangular membrane. As expected, the symmetry of the nodes is reflected in the frequencies at which they form. While the function (185) is depicted as continuous below, it is important to remember that n and m only take on whole integer values. Therefore only certain points of the plane in figure 8 are actually the frequencies at which the nodes occur. For simplicity in visualization we will choose $\alpha = h = l = 1$.

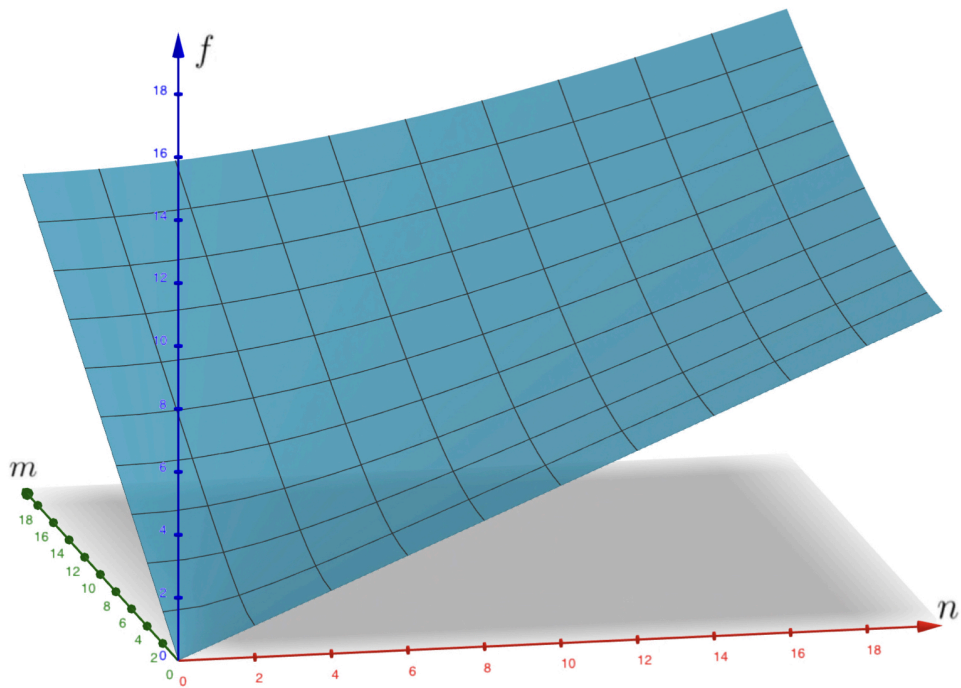


Figure 8: Plane of all vibrational points for a rectangular membrane

However, when we consider the case of the circular plate, the solution is much less intuitive. The solution attained through the procedure shown in section 5 is a seemingly logical one since, similar to the rectangular plate, the nodes are symmetrical and evenly spaced out. However, as shown in section 7, we unfortunately cannot assume that the Chladni figures on a circular membrane are symmetrical in this aspect.

9 Experimental Results

Having been concerned with the mathematical side of Chladni figures for the main part of this paper, it is also important to gather experimental evidence to compare to our theoretical findings. In this section, the steps I took to create Chladni figures are presented. The main goal was to experiment on systems which try to mimic our theoretical models. This means that instead of the rectangular plate, I opted for a rectangular frame with a membrane stretched over it. This configuration was chosen over the classical metal plate, as used by Chladni, for two main reasons: Firstly, it is much easier to fix the boundaries of an elastic membrane and secondly, the membrane vibrates more freely, which makes agitating it possible with a loudspeaker. The vibrations on a metal plate would have to be point driven in order to produce enough resonance for Chladni figures to form, which would not fit our model. For the circular membrane, we used a similar frame in circular form with an attachment point in the center to represent not only the fixed border but also the fixed center point.

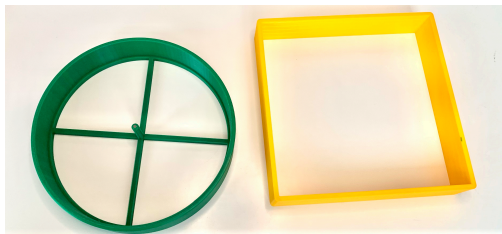


Figure 9: 3D-printed frames

To manufacture the frames shown above, I used the 3D design software "Shapr-3D" in order to create the models. These were then printed on my Prusa i3 MK3 3D printer in yellow and green PLA plastic. Finally a rubber sheet was stretched over the frames and some salt was sprinkled on the membrane. By then placing a speaker, connected to a frequency generator, under the frames, I was able to agitate the membranes which would then hopefully produce Chladni figures.



Figure 10: My only successful Chladni figure with the 3D-printed frames

The process was partially successful. Unfortunately, the figures formed were very irregular due to the mass of the salt, which would lead to the salt accumulating in certain areas and dampening the vibrations at those points, thus creating unwanted nodes. Unfortunately, finer powders such as flour and powdered sugar also exhibited this behavior. Another problem was to stretch the membrane evenly over the frame to obtain a uniform surface tension. Therefore, I was unable to reliably create useful Chladni figures using this method.

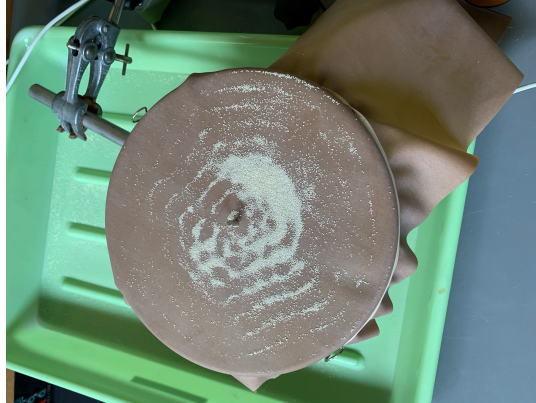


Figure 11: A model example of uneven tensioning

To solve the problem of uniform surface tension, I next attempted to use a drum as the vibrating surface. By weighing down the frames on the top of the drum, I would create the fixed boundaries from our theoretical models. Unfortunately, the mass of the grains still influenced the outcome of the experiment.

I did however notice that at the frequencies at which the nodes should occur according to equation (185), the pitch made by the vibrating drum head would grow considerably louder, suggesting resonance and thus, the formation of nodes. I therefore attempted to use a stretched plastic bag instead of the rubber membrane. Since the plastic bag membrane was lighter and easier to excite, the speaker had little trouble moving the sand grains. Thus, after many hours of trial and error, I obtained the Chladni figures shown in the following section.

9.1 Results from the Circular Membrane

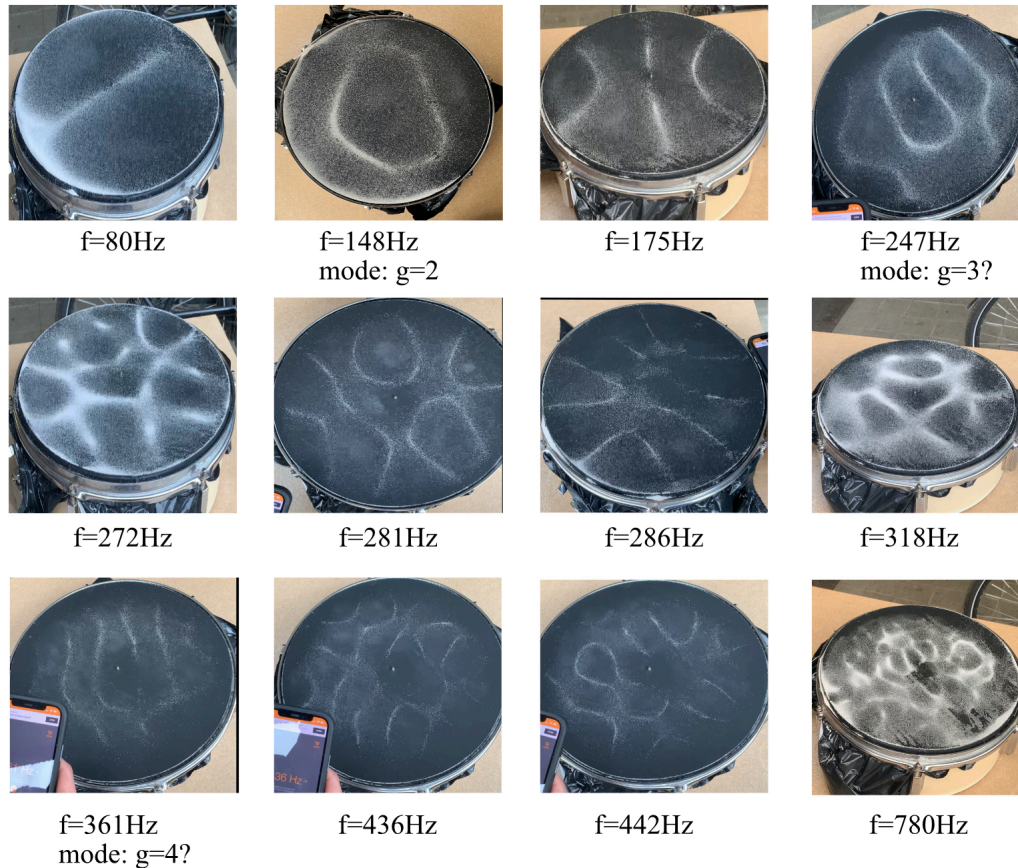


Figure 12: Figures obtained on the circular membrane

As we can observe in the above figure, the Chladni figures turned out quite nicely on the drumhead. Unfortunately, it is difficult to predict most of the figures above using our mathematical model. This may be attributed to external factors, which are not accounted for in our formula. Furthermore, if we assume the mode for $g = 2$ to be correct, we can calculate the wave propagation speed α using equation (131) where f_g denotes the number of the mode:

$$f_g = \frac{g\alpha}{2r}, \quad (186)$$

which, rearranged for α , becomes:

$$\alpha = \frac{2f_g r}{g}. \quad (187)$$

Since we can measure the values $f_2 = 148\text{Hz}$, $r = 0.15\text{m}$ and $g = 2$ we obtain:

$$\alpha = \frac{2 \cdot 148\text{Hz} \cdot 0.15\text{m}}{2} = 22.2 \frac{\text{m}}{\text{s}}. \quad (188)$$

We can now calculate the expected frequencies for $g = 3$ and $g = 4$:

$$f_3 = 222\text{Hz} \quad (189)$$

and

$$f_4 = 296\text{Hz} \quad (190)$$

When we compare these frequencies to the ones of the suspected third and fourth mode in figure 12, we will see that they do not coincide, which discards the supposition. However, we did still obtain a clean second mode which fits with our model for $g = 2$. These results are explainable both through external factors, such as uneven surface tension and non isotropic behavior (among others), and through an incompleteness in my mathematical model from section 5, which has already been shown to be imprecise in section 7. We have also not considered figures which are not rotationally symmetric.

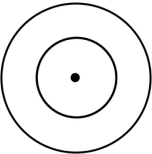
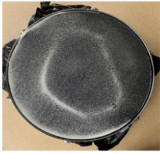
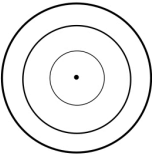

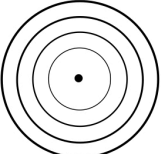

Theoretical Expectation	Experimental Result
 <p>f=148 Hz mode: g=2</p>	 <p>f=148Hz mode: g=2</p>
 <p>f=222 Hz mode: g=3</p>	 <p>f=247Hz mode: g=3?</p>
 <p>f=296 Hz mode: g=4</p>	 <p>f=361Hz mode: g=4?</p>

Figure 13: Comparison of the theoretical and experimental Chladni figures according to section 5

9.2 Results from the Rectangular Membrane

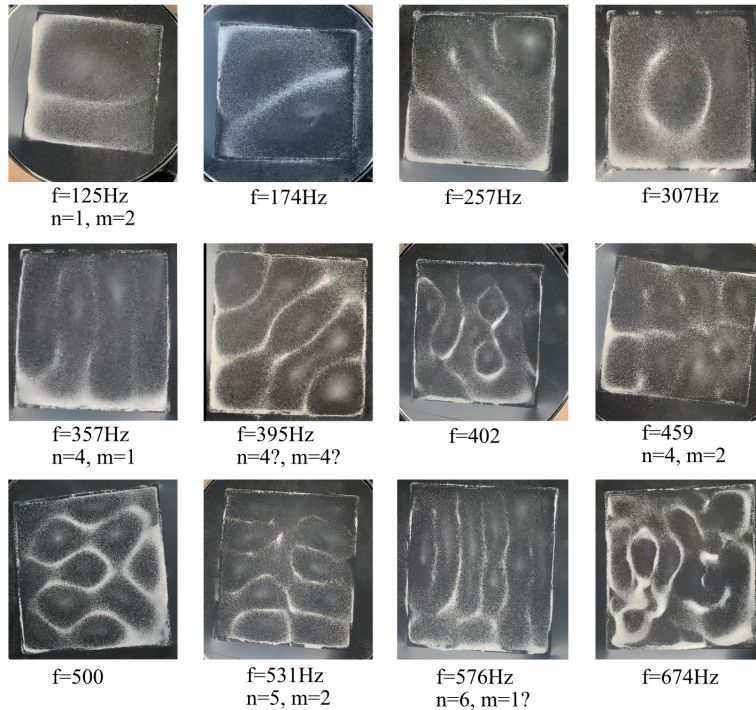


Figure 14: Figures obtained on the rectangular membrane

Although we also cannot describe a large part of the nodal figures on a rectangular plate using the mathematical model for a rectangle, our predictions are significantly better than on the circular plate. Similar to the previous section, we can figure out the wave propagation speed α by assuming that one of our figures is correct through equation (186):

$$f_{n,m} = \frac{\alpha}{2lh} \sqrt{n^2h^2 + m^2l^2} \quad (191)$$

By assuming that our results for $f_{5,2}$ are correct, we obtain:

$$\alpha \approx 37.47 \frac{\text{m}}{\text{s}} \quad (192)$$

This gives us the following interesting predictions:

$$f_{1,2} \approx 220\text{Hz} \quad (193)$$

$$f_{4,1} \approx 406\text{Hz} \quad (194)$$

$$f_{4,2} \approx 440\text{Hz} \quad (195)$$

$$f_{4,4} \approx 558\text{Hz} \quad (196)$$

$$f_{6,1} \approx 599\text{Hz} \quad (197)$$

If we compare these values with figure 14, we can see that, despite not being precise, the frequencies are in a similar range as the frequencies shown. However for (197), our guess that this figure has the mode $n = 4, m = 4$ is probably wrong. The imprecision of our results is certainly the direct consequence of both an incomplete model and external factors influencing the experiment, which have not been accounted for in the model.

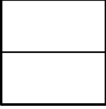
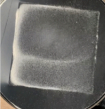
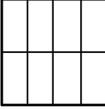
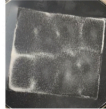
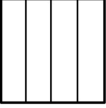
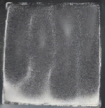
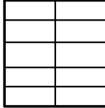
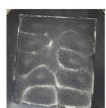
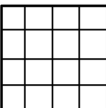
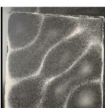
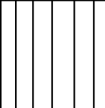
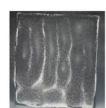
Theoretical Expectation	Experimental Result	Theoretical Expectation	Experimental Result
 $f=220\text{ Hz}$ $n=1, m=2$	 $f=125\text{Hz}$ $n=1, m=2$	 $f=440\text{ Hz}$ $n=4, m=2$	 $f=459$ $n=4, m=2$
 $f=406\text{ Hz}$ $n=4, m=1$	 $f=357\text{Hz}$ $n=4, m=1$	 $f=531\text{ Hz}$ $n=5, m=2$	 $f=531\text{Hz}$ $n=5, m=2$
 $f=558\text{ Hz}$ $n=4, m=4$	 $f=395\text{Hz}$ $n=4?, m=4?$	 $f=599\text{ Hz}$ $n=6, m=1$	 $f=576\text{Hz}$ $n=6, m=1?$

Figure 15: Comparison of the theoretical and experimental Chladni figures on a rectangular membrane

10 Chladni Figures in Lutherie

As hinted in the introduction, Chladni figures find a very niche application in the world of violin construction [Appendix]. When a violin resonates, the top and bottom plates vibrate. If one were to spread sand on the plates, one would observe nodal patterns while playing the instrument. In our calculations, we have had to make many approximations in areas such as isotropy and membrane thickness. However, when constructing a violin, these neglected factors are the ones which have the biggest influence on the resonance of the instrument and as such, on the Chladni figures formed. Since the figures and the sound of the instrument stand undoubtedly in some sort of correlation, there exists a method to measure the nodal patterns on a violin. By measuring the vibrations using lasers in a tight, grid like array, one is able to find the nodes by finding the points where the plate does not vibrate. This technique is aptly named modal analysis.

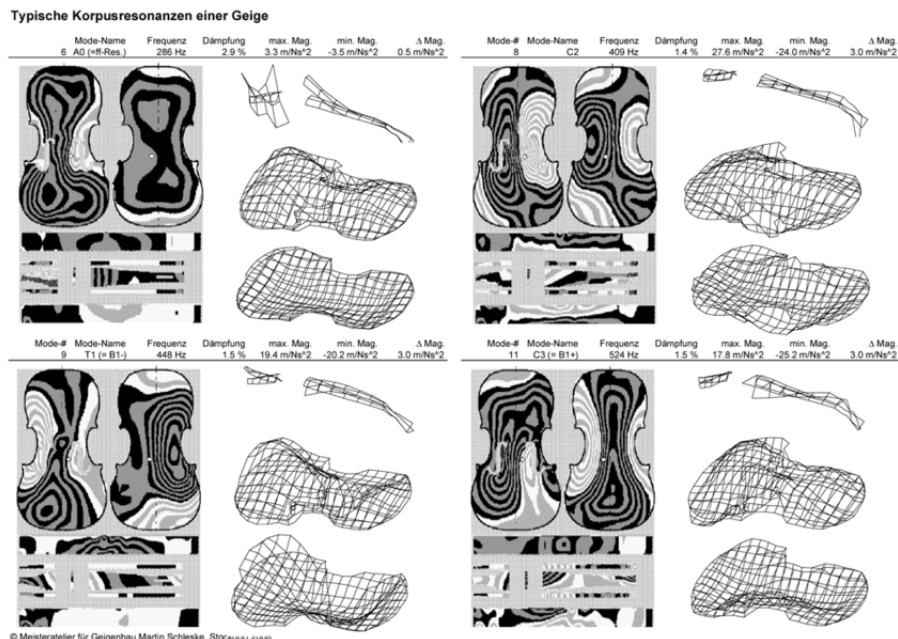


Figure 16: Typical results of a modal analysis on a violin [6]

In the above figure, the column to the left shows the vibrating front and back plates using contour lines to denote areas with the same amplitude and the right side shows an exaggerated model of the resting plates curvature.

Unfortunately, this method currently only finds limited usage in the violin world, but it holds enough potential to be a promising technique used to check parameters such as optimal wood quality and thickness throughout the plate. The largest problem with modal analysis is that it can only measure the nodal patterns up to frequencies of approximately 800 Hz. Current devices are not advanced enough to capture more intricate, high frequency patterns. Thus, the modal analysis is only able to predict the low frequency characteristics of the violin. By looking at the different modes, it is possible to tell if the violin will have a "dark" or "bright" sound. Unfortunately, there are excellent instruments in both of these categories. Rather, the quality of the violin is determined by its resonance with higher harmonics in the frequency range above 800 Hz.

Another interesting application of these nodal figures could be in lutherie schools. Since an apprentice luthier does not have extensive expertise, it can sometimes be difficult to fabricate an even violin plate. Therefore, by analyzing the modes on the apprentice's plate, it would be possible to give direct and visual feedback on what modifications need to be made in order to improve its resonance.

11 Conclusion and Improvements

In this paper, we have attempted to mathematically describe the formation of Chladni figures on a circular and rectangular membrane, discussed possible inaccuracies in our mathematical descriptions, created our own figures in the lab and finally, we have shown some applications of Chladni figures in lutherie. For a rectangular membrane, we obtained the following formula governing the formation of Chladni figures:

$$u(x, y, t) = \sin\left(\frac{n\pi x}{l}\right) \sin\left(\frac{m\pi y}{h}\right) \sin\left(t\pi\alpha\sqrt{\frac{n^2}{l^2} + \frac{m^2}{h^2}}\right), \quad (198)$$

where n is the number of nodes in the x direction without counting the node at $x = 0$, m is the number of nodes in the y direction without counting the node at $y = 0$, l is the length of the plate in the x direction, h is the height of the plate in the y direction and α is the wave propagation speed in the membrane.

For a circular membrane, our formula states that

$$u(x, y, t) = \sin\left(\frac{g\pi x}{\cos\left((2k-1)\frac{\pi}{2^n}\right) \cdot \frac{r}{\cos\left(\frac{\pi}{2^n}\right)}\right) \sin\left(\frac{g\pi y}{\sin\left((2k-1)\frac{\pi}{2^n}\right) \cdot \frac{r}{\cos\left(\frac{\pi}{2^n}\right)}\right) \cdot \sin\left(\frac{g\pi\alpha t}{\sqrt{\left(\cos\left((2k-1)\frac{\pi}{2^n}\right) \cdot \frac{r}{\cos\left(\frac{\pi}{2^n}\right)}\right)^2 + \left(\sin\left((2k-1)\frac{\pi}{2^n}\right) \cdot \frac{r}{\cos\left(\frac{\pi}{2^n}\right)}\right)^2}}\right), \quad (199)$$

where g is the number of radial nodes, r is the radius of the circle, n is the number of vertices of the 2^n -gon, α is the wave propagation speed and k is the the numerator of the vertices varying between 1 and n . As n goes towards infinity, the 2^n -gon takes on a more and more circular shape. This is a hybrid of a one dimensional and two dimensional solution, which gives the placement of the nodes as well as the frequency at which they occur.

Equation (199), however, contradicts our findings from the wave equation in Polar coordinates:

$$R(r) = \sum_{k=0}^{\infty} \frac{(-1)^k}{(2^k \cdot k!)^2} ((r + Q_1)\lambda^2)^k. \quad (200)$$

This equation is an infinite polynomial, where r is the radius of the circle, Q_1 is the numerically determined first root of the function, k is a positive integer, and λ is a constant.

As shown in section 9, the mathematical models do not correspond particularly well to the experimental results. Reasons for these incoherences

are most probably external influences not taken into account in the formula, such as uneven surface tension, thickness, material and temperature of the membrane, as well as the negligence of the mass and grain size of the sand. It is also probable that the mathematical model is incomplete. Possible improvements could include better quality membranes and frequency generators with, eventually, a more direct way of agitating the membrane. Access to more sensitive instruments would have also enabled the modal analysis of more complex shapes such as a violin plate. Also, a numerical analysis of the two dimensional partial differential equation could lead to the prediction of some Chladni figures which are not able to be seen in our models.

12 Personal Reflection

By taking on this mathematical journey, I have learned two seemingly opposite things about the nature of science and mathematics. Firstly, math is hard. It requires a distinct will as a novice, to question, research and try out various solution methods, most of these not leading to a fruitful end. I started with the grandiose idea that I may be able to predict Chladni figures on an actual violin. I was looking forward to comparing my model with experiments on my own instrument. I had hoped to find out how I could use the patterns to judge the quality of the sound.

Applying mathematics to describe physical phenomena is not always as straightforward as it may seem. Unfortunately, the irregularities in the shape of a violin make it virtually impossible to describe at this level using just a pen and some paper. Thus, I had to greatly simplify my mathematical goal, down to an overly idealized membrane. Additionally, I now sit here, after doing hundreds of hours of calculations, research and experiments, just to find out that what I spent so much time and energy doing, does not predict most of the experimental results and cannot even be used reliably in violin building. This is the first thing I learned: the mathematics hidden in nature is not always visible right away. We are not simply allowed to neglect certain factors and expect our results to match real world phenomena. However, through simplification we can break down nature's mountains of intricacy into manageable bricks. Stone by stone, we can use these building-blocks to slowly construct our knowledge and understanding of the universe.

Secondly, although math is hard, I truly enjoy it. I learned how to dive deep into the ocean and more importantly, how to hold my breath once down there. In other words, I learned to dare to grasp my way in the dark, to

approach subjects that seem daunting at first and I learned how to persist, to not give up when something doesn't work out. I threw myself again and again at the wall which was this project, like waves upon the cliffs, until I found a small crack in the barricade. Sometimes, I would need a nudge in the right direction, but eventually, I found the way through, no matter how small the opening. Then, by trying and trying again, I would slowly widen the gap, understanding more and more about what was waiting on the other side until at some point, I came crashing through. There are few things more pleasing than getting a satisfying solution to a problem. Seldom was I more proud than when I managed to describe with mathematics what my eyes could see.

Acknowledgements

I would like to wholeheartedly thank my supervisor Yee Ling Willems-Ong for supporting me throughout this mathematical journey. Through her endless expertise and investment, she was able to teach me the tricks of the trade and truly showed me what writing a physics paper is all about. Her passion for the subject has left a lasting imprint, which I will hopefully never forget.

I would also like to thank the lab technicians at the Kantonsschule Rämibühl for providing me with equipment and instruments, greatly facilitating my experiments.

Furthermore, I could not have gathered the required information regarding lutherie without the help of world class luthiers Johannes Leuthold and Stephan-Peter Greiner.

I would also like to thank the percussion section of the Tonhalle Orchester Zürich for sacrificing a snare drum in the name of science.

Finally, I would like to thank my parents for putting up with my endless rambling on partial differential equations and more importantly, for helping me carry out and troubleshoot my experiments.

References

- [1] Boyce, William E. and DiPrima, Richard C. (1986). Elementary Differential Equations and Boundary Value Problems. P. 114.
- [2] Schleese, Torsten and "Wochen" (2021). Ernst Florens Friedrich Chladni.

https://de.wikipedia.org/wiki/Ernst_Florens_Friedrich_Chladni
(2.12.2021)
- [3] Figure 2: Morris, Stephen (2009). Violin shaped Chladni plate at 1452.3 Hz.

<https://www.flickr.com/photos/nonlin/3861695693> (10.11.2021)
- [4] Figure 3: Lee, Kevin (2010). Violin making.

https://kevinleeluthier.com/violinmaking/making_1.htm (10.11.2021)
- [5] Figure 5: Collins, Danielle (2019). Motion basics: Difference between Cartesian and polar coordinate systems.

<https://www.linearmotiontips.com/motion-basics-difference-between-cartesian-and-polar-coordinate-systems/> (10.11.2021)
- [6] Figure 16: Schleske, Martin (Unknown). Violin Acoustics - Modal analysis.

<https://www.schleske.de/en/research/introduction-violin-acoustics/modal-analysis/results.html> (10.11.2021)
- [7] "AashiK" (2019) Deducing the wave equation in polar coordinates.

<https://www.sarthaks.com/420830/deduce-the-two-dimensional-wave-equation-in-polar-coordinates-r> (1.11.2021)

Appendix: Interview with Stephan Peter Antwort

Frage: "Was kann man von der Modalanalyse lernen?"

"Antwort: Wir verstehen mehr wie die Bewegung von Boden und Decke in den tiefen Frequenzen funktioniert und können damit auch lernen wie wir die Parameter: Wölbung, Holzdicke und Holzmaterial aufeinander abstimmen können damit wir entsprechende chladnische Klangfiguren (Moden) erhalten die die entsprechenden Bilder bei den entsprechenden Frequenzen haben."

Frage: "Was kann man nicht damit lernen?"

Antwort: "Soweit ich weiss, wird es ab 800 Hz nach oben schwierig Moden eindeutig zu bestimmen, das heisst alles was darüber liegt, können wir über die Modalanalyse nicht sehen und nicht verstehen und für mich persönlich sind das die eigentlich wichtigen Frequenzen über 800Hz. Das heisst was sich darüber abspielt unterscheidet erst die gute von der schlechten Geige. Das heisst wir können unterhalb von 800Hz ein bisschen den Klangcharakter feststellen, ob eine Geige dunkel oder hell ist, was aber dann vor allem auf der G und D Saite relFraget ist. Wie gesagt wir können den Charakter aber nicht die Qualität der Geige feststellen. Wenn eine Geige nicht dunkel ist, heisst das nicht, sie ist schlecht, sondern sie kann auch nicht dunkel aber fantastisch gut sein."

Frage: "Kann die Modalanalyse in Geigenbauschulen als Lernmittel verwendet werden?"

Antwort: "Ich denke wenn man sie (Modalanalyse) versteht und auch die Grenzen davon kennt und das den Schülern vermittelt, kann man da viel machen, weil es gerade in dem Grundtonbereich der Geige möglich ist das Verhalten der Geige baulich zu beeinflussen. Das heisst wir können über die Parameter: Holzmaterial, Wölbung und Holzdicke/stärke können wir tatsächlich aktiv beeinflussen. Wir können sagen wir machen die Geige ein bisschen dunkler indem wir sie ein bisschen dünner machen beispielsweise und können das sehr gut über die Modalanalyse kontrollieren. Als Geigenbauer hätte man im grunde genommen die Möglichkeit des ganz einfachen Biegens der Platte, dann kann man feststellen wie weich ist sie. Wir können aber auch über die Modalanalyse feststellen ob die Weichheit die richtige ist. Das ist ein toller Lerneffekt an der Geigenbauschule."

Frage: "Welche Zukünfte bieten sich für die Modalanalyse?"

Antwort: "Weil die Modalanalyse letztendlich die Art und weise wie die Platten schwingen, wie es sich bewegt beschreibt, hat es natürlich auch eine Aussage über über die hohen Frequenzen. Das heisst wenn wir es erreichen können die Modalanalyse für hohe Frequenzen auch anwenden zu können und wir einen zuverlässigen Zusammenhang zwischen dem wie eine Platte sich bewegt, was die Modalanalyse ja angibt, und wie die Geige abstrahlt finden, dann würden die Aussagen über wie sich die Platte bewegt durch Modalanalyse auch eine verlässliche Aussage über die Abstrahlcharakteristik auch in den hohen Frequenzen machen, was sehr wertvoll wäre. Da ist man aber noch nicht. Es ist logisch, der Grund der Abstrahlung ist die Bewegung der Platte, das heisst so wie die Platte sich bewegt, so irgendwie steckt die Information der Abstrahlung auch drin, das ist einfach noch nicht so richtig hergestellt. Dieses Bindeglied. Letztendlich interessiert es den Hörer nicht wie sich die Geige bewegt, sondern wie sie abstrahlt."